

## ***Supporting Information***

### **Density Gradient Strategy for Preparation of Broken In<sub>2</sub>O<sub>3</sub> Microtubes with Remarkably Selective Detection of Triethylamine Vapor**

Wei Yang,<sup>†</sup> Liang Feng,<sup>‡</sup> Saihuan He,<sup>†</sup> Lingyue Liu,<sup>†</sup> Shantang Liu<sup>\*,†</sup>

<sup>†</sup>Key Lab for Green Chemical Process (Ministry of Education), School of Chemistry and Environmental Engineering, Wuhan Institute of Technology, Wuhan 430205, P. R. China.

<sup>‡</sup>Key Lab of Separation Science for Analytical Chemistry, Dalian Institute of Chemical Physics, Chinese Academy of Sciences (CAS), Dalian 116023, P. R. China.

\*Corresponding author: (E-mail) stliu@wit.edu.cn

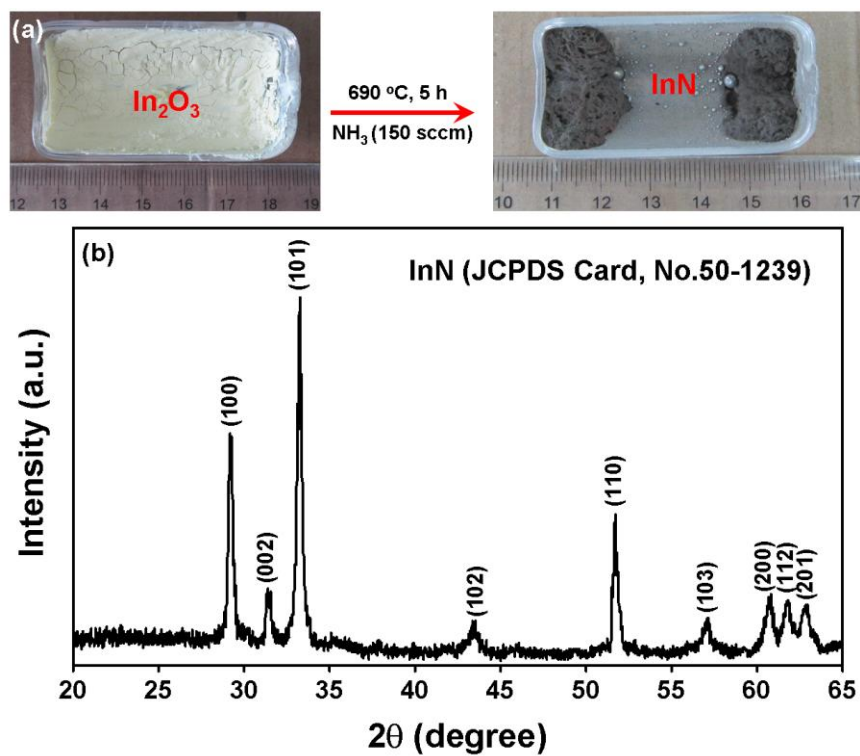


**Figure S1.** (a) Commercial  $\text{In}_2\text{O}_3$  onto quartz boat before and after the ammonia treatment; (b) XRD pattern of the as-obtained sample after the ammonia treatment.

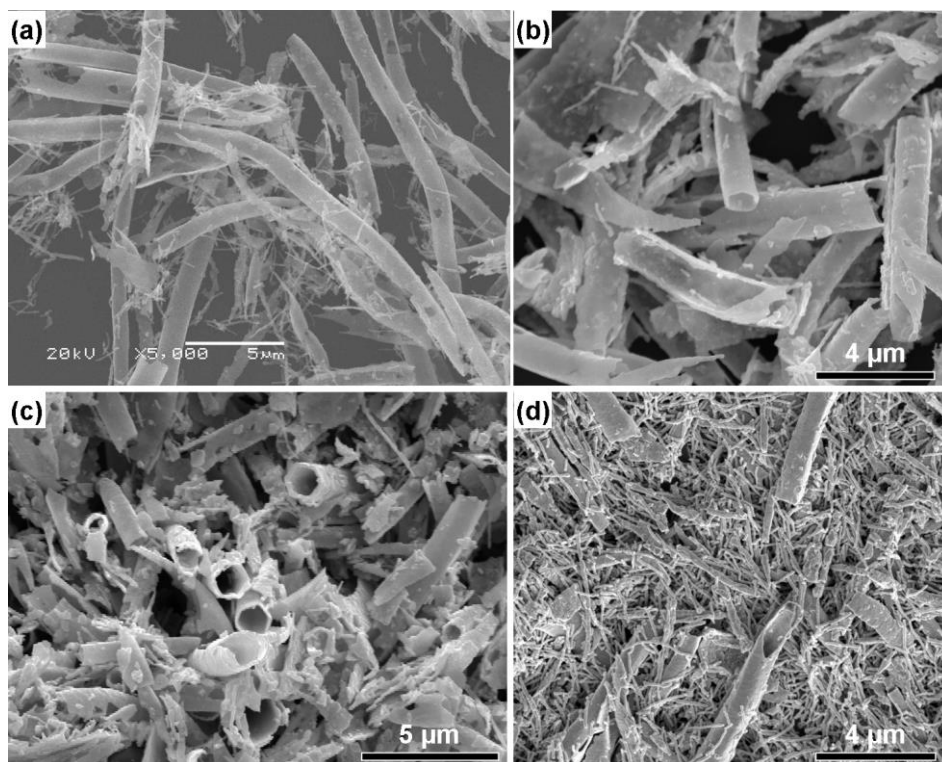


**Figure S2.** SEM images of  $\text{In}_2\text{O}_3$  products under various centrifugation speed and time: (a) 1000 rpm for 10 min; (b) 1500 rpm for 8 min; (c) 2000 rpm for 5 min; (d) 3000 rpm for 3 min.

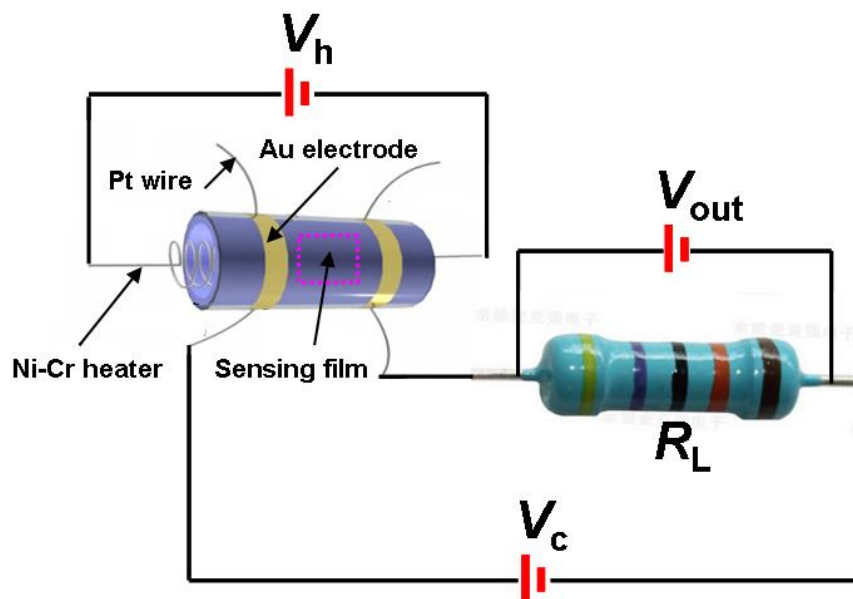


**Figure S3.** Schematic diagram for the measurement and configuration of gas sensor.

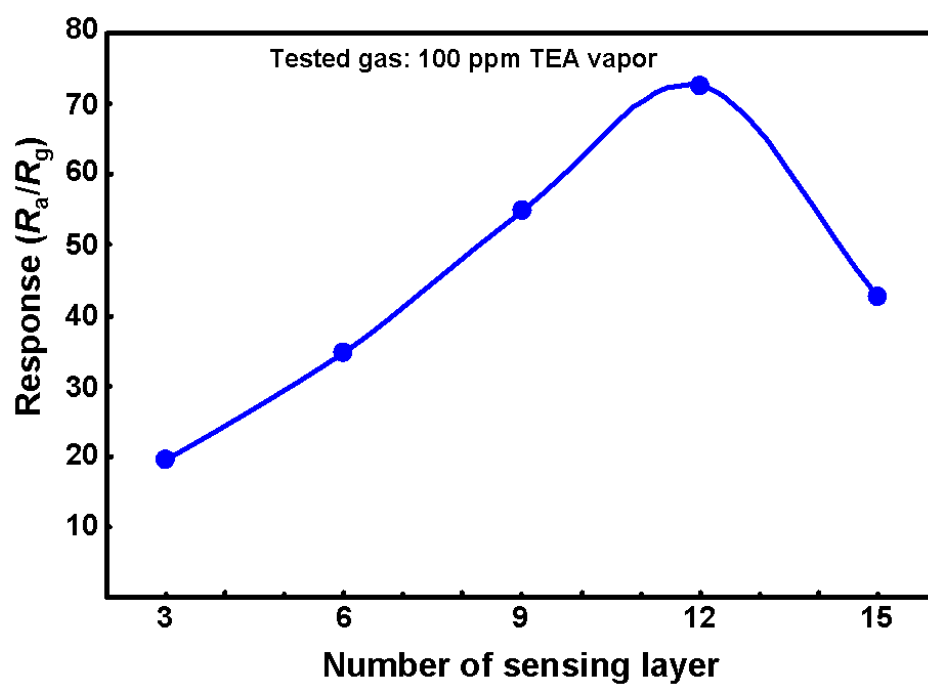


**Figure S4.** Sensor response based on the broken  $\text{In}_2\text{O}_3$  microtubes versus thickness of sensing layer.

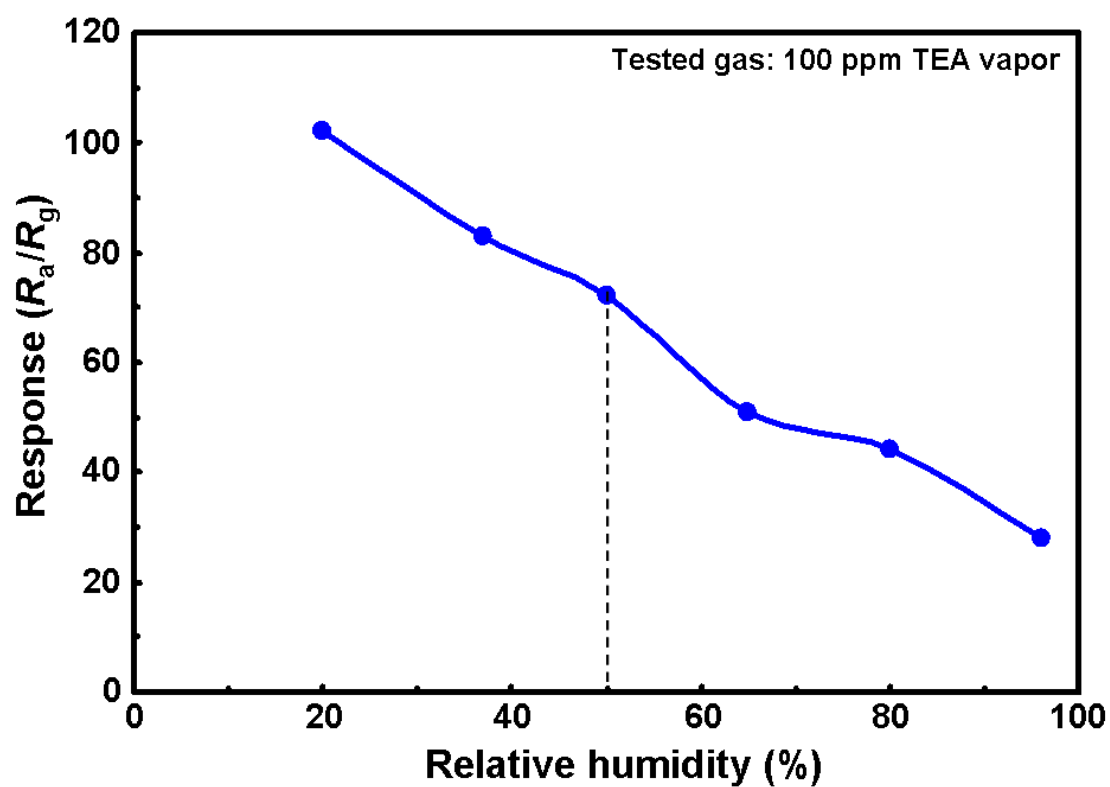


**Figure S5.** Sensor response based on the broken  $\text{In}_2\text{O}_3$  microtubes under various RHs.

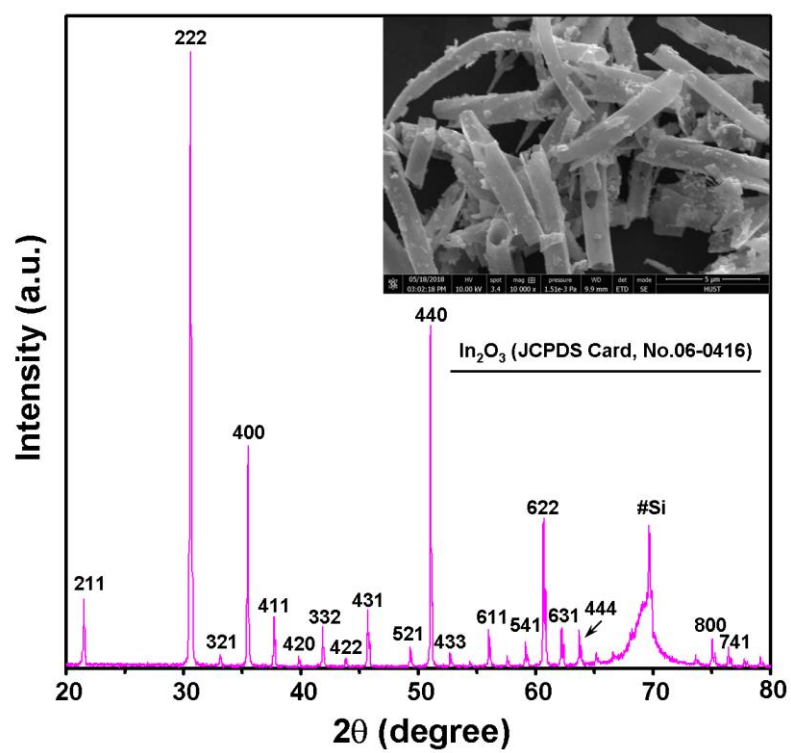


**Figure S6.** XRD pattern and SEM image (inset) of the  $\text{In}_2\text{O}_3$  microtubes after the sensing measurements.

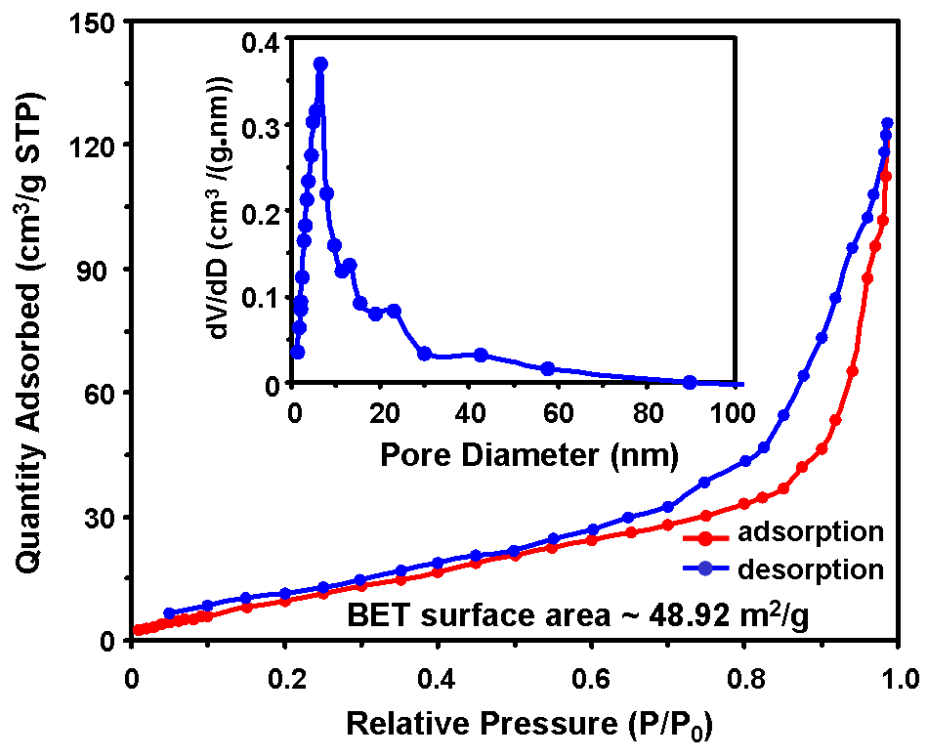


**Figure S7.** Typical nitrogen adsorption-desorption isotherm and the corresponding pore-size distribution of the  $\text{In}_2\text{O}_3$  microtubes after the sensing measurements.